Evaluation of Necessary Delay before Inspection for Hydrogen Cracks

Postweld crack development was monitored over time on a variety of test welds

BY R. PARGETER

Introduction

In the welding of ferritic steels, the most common form of fabrication cracking is that caused by hydrogen embrittlement. It is well known that there can be some delay between the completion of welding and the formation of hydrogen cracks in ferritic steels. Therefore, if inspection is carried out too soon after welding, these cracks may not be detected, with potentially catastrophic consequences. On the other hand, excessive delays after welding prior to inspection can have serious financial implications due to, for example, holdups in production.

Currently, there are recommendations for delays of between 16 and 48 hours in various national and industry standards (Refs. 1–5), but there is no firm basis for these times. Furthermore, there is generally no discrimination between different materials, joint geometries, or welding conditions, with just one delay time recommended for all circumstances.

It was against this background that a program of experimental work was initiated in which crack development was monitored using ultrasonic techniques in a variety of test welds.

Background

It is well established that hydrogen cracking in ferritic steels only occurs when a critical combination of the four basic factors involved is exceeded. These factors are

1) Hydrogen
2) Susceptible microstructure
3) Tensile stress
4) Temperature.

The likelihood of cracking increases with increasing hydrogen level, microstructural susceptibility, tensile stress, and as the temperature approaches about 20°C (68°F). In the final stages of cooling following welding, three of these parameters are slowly changing, as depicted schematically in Fig. 1. Even when cooling has stopped, however, and the developed contraction stresses have stopped increasing, the hydrogen content will continue to change. For the weld as a whole, the hydrogen level will decrease as a result of diffusion out of the weld metal and heat-affected zone (HAZ) and the adjacent base material. However, at local points within the weld metal and HAZ, particularly those of high triaxial stress, the hydrogen content will increase for a period of time as a result of stress-assisted diffusion. Hydrogen will diffuse up stress gradients from regions of *lower* to *higher* concentration. Thus, it could be some time after completion of welding and cooling that, locally, the hydrogen concentration first reaches a critical value and cracking commences. This effect of hydrogen diffusion was noted as early as 1961 when Beacham et al. (Ref. 6) demonstrated that cracking in Lehigh restraint tests could be delayed by storing test panels at low temperatures. In their tests, they found that cracking occurred between one-quarter and one-half hour after welding under normal conditions. For similar welds quenched to –110°F immediately after welding, cracking was suppressed during storage at –110°F but did occur approximately one-quarter hour after reaching room temperature again. Hydrogen diffusion is therefore one feature that can contribute to the observed delayed nature of hydrogen cracking.

A further aspect contributing to the delay is due to the fact that hydrogen cracking is frequently of a discontinuous nature. In part, this also arises from the stress-dependent diffusion characteristics of hydrogen since, as the crack moves forward, it enters a region of locally lower hydrogen concentration and an "incubation time" is then required for the hydrogen concentration to increase locally, by stress-assisted diffusion, at the new point of maximum stress near the new crack tip. Andersson (Ref. 7) suggests that an additional explanation for the time delay could be the formation of hydrogen traps, e.g., voids, dislocations, etc., at the crack tip by plastic straining, which temporarily lower the lattice hydrogen concentration. A third aspect, which plays a part in the often observed delayed nature of hydrogen cracking, relates to the time required for hydrogen cracks, once formed, to grow to a sufficient size to be detected by the NDE method being applied.

For a given weld, the delay time can be seen to be primarily a function of the combined magnitude of the three parameters (hydrogen level, microstructural susceptibility, and stress) in relation to the required critical combination. When the combined values of these are at very high levels, i.e., the welding procedure has a very high risk of cracking, cracking may commence well before cooling to normal ambient temperature is completed. On the other hand, the likelihood of a delayed characteristic is greatest when the combination of factors involved in producing hydrogen cracking are only marginally above the critical combined value, and this is achieved only by the local enhancement of hydrogen through stress-assisted diffusion. Hydrogen level is clearly an important variable influencing delay time since it is well established from constant load or stress rupture tests (Ref. 8) that, as the hydrogen concentration decreases, this leads to longer incubation times for rupture. Ultimately, of course, continued lowering of the bulk hydrogen concentration leads to a situation where, no matter how long a wait is imposed, local enhancement of hydrogen concentration by stress-induced diffusion cannot obtain the critical level before overall loss of hydrogen results in the local hydrogen level beginning to decline.

Other factors that are likely to increase the delay time over and above those that contribute to a marginal procedure will be those that prolong the time during which local hydrogen concentrations can increase and stay close to critical concentra-

KEY WORDS

Embrittlement
Fabrication Cracking
Hydrogen Cracking
Stress-assisted Diffusion
Ultrasonic Inspection

R. PARGETER is Consultant, Ferritic Steels and Sour Service, Metallurgy, Corrosion, Arcs & Surfacing Technology Group, TWI Ltd., Cambridge, U.K.

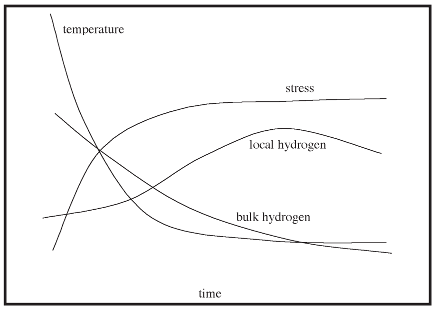

Fig. 1 — Schematic indication of how stress, temperature, and hydrogen levels change with time after completion of welding.

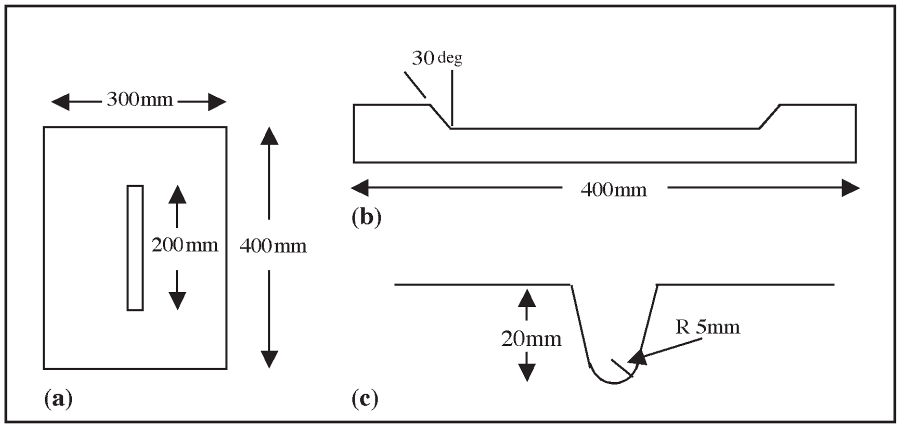

Fig. 2 — Dimensions of groove weld test panels.

tions, or those that enhance the stress-induced diffusion. Thus both high joint thickness and high restraint levels could be expected to be important factors. Thickness is important because bulk hydrogen concentration will decay only very slowly at the center of thick sections, while high restraint is important because higher stresses could increase the extent of locally enhanced hydrogen through stress-induced diffusion. Furthermore, the delay time can be expected to be some function of the diffusion rate of hydrogen in steel, which, at room temperature, can vary by at least two orders of magnitude (Ref. 9) with material conditions, compositions, and cleanliness; the slower the diffusion rate, the slower the overall loss of hydrogen will be and the longer the time for stress-induced diffusion to locally achieve critical hydrogen levels. Finally, it is possible that the crack location (buried or surface breaking) will influence delay time because hydrogen concentrations in near-surface regions will decay more rapidly. In addition, a surface-breaking crack will itself provide a conduit for hydrogen escape.

Experimental Approach

Multipass welds in butt joints were made in a variety of steels, and the development of hydrogen cracking was monitored using mechanized ultrasonic examination in which constant coupling was ensured. For the majority of the work, welds were stop-ended bead in groove, in 50-mm- (2-in.-) thick plate. Using this basic geometry, effects of base metal and welding consumable, heat input, hydrogen level, and restraint were explored using shielded metal arc welding. Some trials were also carried out at higher heat input using larger submerged arc welded butt joint panels.

As explained in the previous section, the greatest delays between completion of welding and cracking are anticipated at near-threshold conditions. Thus, for each of the above factors, a series of welds around threshold conditions was made. In C-Mn steels, this was achieved principally by varying heat input, and in alloy steels by varying preheat.

Experimental Details

Materials and Welding

Details of base materials are presented in Table 1. Four C-Mn steels were used, two with 350-MPa (51-ksi) specified minimum yield stress (SMYS), and two with 450-MPa (65-ksi) SMYS. The two 350-MPa steels were fairly closely matched in chemical composition, with the exception of S, Si, and O — one being a clean steel (<0.002% S, 0.0004% O) and the other fairly dirty (0.037% S, 0.0035% O). The 450-MPa steels were clean (≤ 0.003% S, 0.0009% O). Carbon equivalent levels (0.38–0.45%) were selected to help with generation of cracking. One low-alloy steel with SMYS of 690 MPa (100 ksi) (grade HY100) was used, and a limited number of tests were carried out on some 565-MPa (82-ksi) yield HSLA steel (grade Q1N).

Shielded metal arc consumables used were E7018 for 350- 1MPa yield steel, E8018G for 450-MPa yield steel, E9016G for the Q1N steel, and E12018MM for the HY100 steel. An SD3 wire was used for submerged arc welding 350-MPa yield steel, and an SD3 1Ni-¼Mo wire for 450-MPa yield steel.

Shielded metal arc consumables, with the exception of E9016G and E12018MM, were supplied in part-dried condition, thus allowing them to be dried to a required hydrogen level, between about 4 and 12 mL/100 g deposited metal. A part-dried basic agglomerated flux was used for submerged arc welding, dried as required to give between about 8 and 13 mL/100 g deposited metal. Typical weld metal chemical compositions are given in Table 2.

The dimensions of welded groove and butt-joint test panels are shown in Figs. 2 and 3. In both cases, a good surface was required to facilitate automated ultrasonic inspection from the weld root side. The groove samples were machined flat at the same time the groove was machined, and for the welded butt-joint panels, the backing bar was machined off after completion of the root pass. Variations in the groove panel geometry to provide reduced restraint (through end and side slits), different groove depths, and different groove widths were incorporated in the program. Heat inputs of between about 0.6 and 2.4 kJ/mm were used for shielded metal arc welds in C-Mn steels and between 3.5 and 5 kJ/mm for submerged arc welds. For the tests on the low-alloy (690-MPa yield) steel, all welds were made at a heat input of about 1.1 kJ/mm.

A summary of all the test series is presented in Table 3.

Nondestructive Examination

Details of inspection equipment and techniques developed to some extent throughout the project, but the principles, which aimed to achieve constant and reproducible coupling, remained the same. For the groove welds, coupling was achieved by immersing the specimen in an oil bath — Fig. 4. A pan of fixed probes, providing a combination of longitudinal and transverse pulse echo and time-of-flight diffraction examinations, was automatically traversed over the reverse sides of the specimens. Test samples were immersed in the oil bath when they had cooled to about 40°C adjacent to the weld. The time of the first inspection varied, due to differences in weld cooling times and other experimental variables, between about 30 minutes and 8 hours after completion of welding, generally being between 1 and 3 hours.

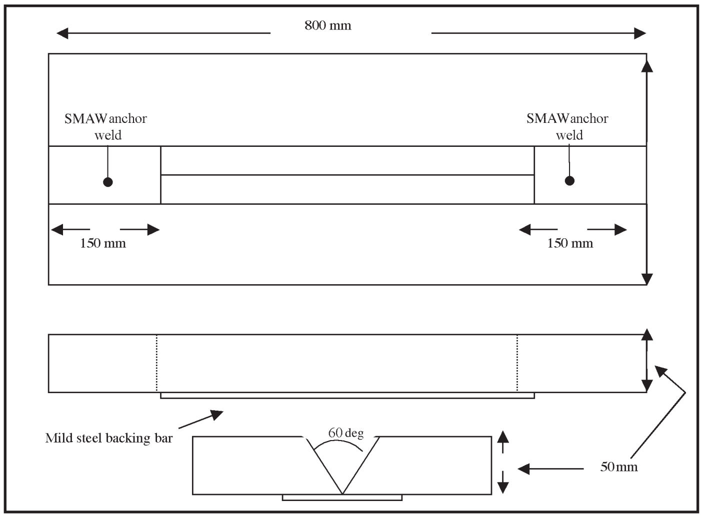

Fig. 3 — Dimensions of welded butt-joint test panels.

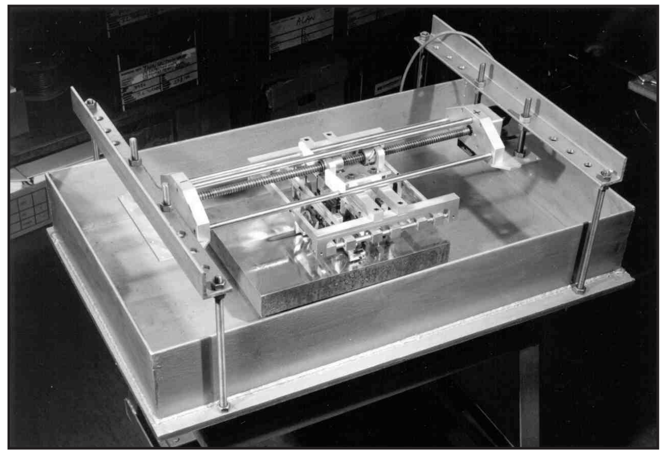

Fig. 4 — Oil bath and ultrasonic inspection equipment used for groove welds.

For the pulse/echo inspections, only indications having an amplitude greater than that from a 3-mm side-drilled hole plus 14 dB were displayed. Thus, the sensitivity was neither lower nor significantly greater than that which is usual in practice. It should be recognized, however, that the detectability of all defects using fixed orientation probes is limited by comparison with a manual inspection. Time-of-flight probes were used to compensate for this and to provide information on crack growth.

Interpretation of pulse/echo signals was complicated by an observed increase in signal amplitude for all reflections, including stable geometrical features such as the weld cap profile, as the weld cooled. Where features were observed on first inspection (by either technique) and none of the observed features changed during subsequent monitoring, their nature was confirmed by metallographic sectioning.

For submerged arc welds, immersion in the oil bath was not possible. For these welds, manually controlled mechanized scans were carried out. A probe pan and stepper motor were attached to the back face of each weld with magnetic feet as soon as it had cooled to about 30°C, and kept in place for the duration of the test. Only time-of-flight probes were used for these inspections.

All inspections were carried out at increasing intervals over a total period of about one week. The initial interval for the automated, oil bath tests was one-half hour, increasing logarithmically to 12 hours at the end of the week. Test intervals on the submerged arc welds were 1 hour for the first 3 hours, every 2 hours for the next 6 hours, every 8 hours for the next 4 days, and, finally, 24 hours until the end of the week.

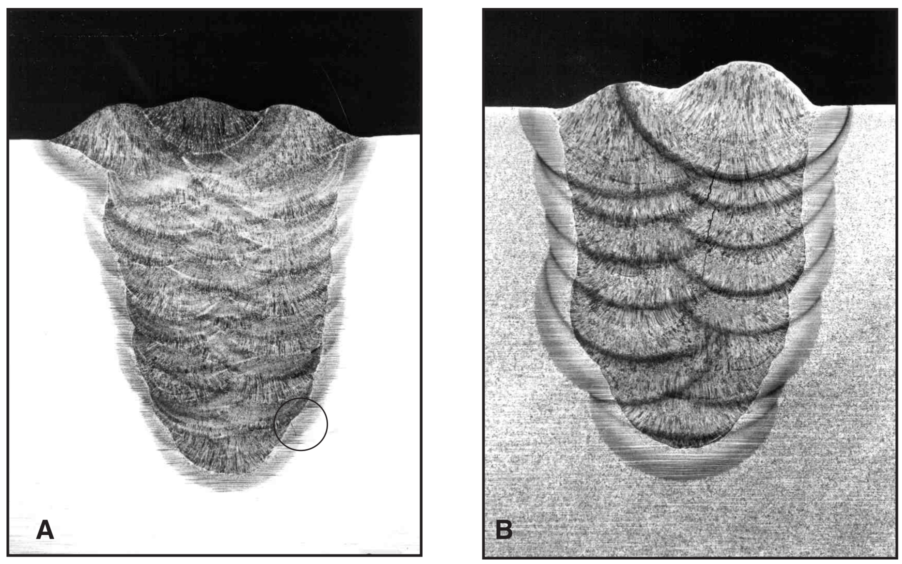

Fig. 5 — Photomacrographs of: A — HAZ crack in W1-14 (low-hydrogen, high-restraint 350-MPa C-Mn steel); B — weld metal crack in W1-2 (low-hydrogen, high-restraint HY100 steel).

Results

Examples of HAZ and weld metal cracks in groove welds are given in Fig. 5. The results of delay time measurements are presented in Table 4. Four principal times were recorded, all relative to completion of welding. These were the time of first inspection, time of first detection of a crack, the last time when a new crack was observed, and the last time when a change in crack size relative to the previous inspection was observed. In addition, some information on cooling is included in this table.

In the parametric studies, exploring the effects of restraint, hydrogen level, and groove depth at approximately constant heat input, in the 350-MPa yield steel, hydrogen cracking (when it occurred) was always present at the time of first inspection. Growth of existing subsurface HAZ cracks was observed for up to 6 hours after welding in the high-restraint welds at both high and low hydrogen levels (e.g., W1-20 and W1-10). Although such growth was not detected in low-restraint welds, it was not possible to conclude that any of restraint, hydrogen level, or weld thickness over the ranges studied had any effect on delay time.

The results of these parametric studies on the HY100 (690-MPa yield) steel, however, showed many instances of measurable delays in both initiation and growth of weld metal hydrogen cracks (Table 4 and Figs. 6–9). When examining these data, it should be recognized that for W1-15

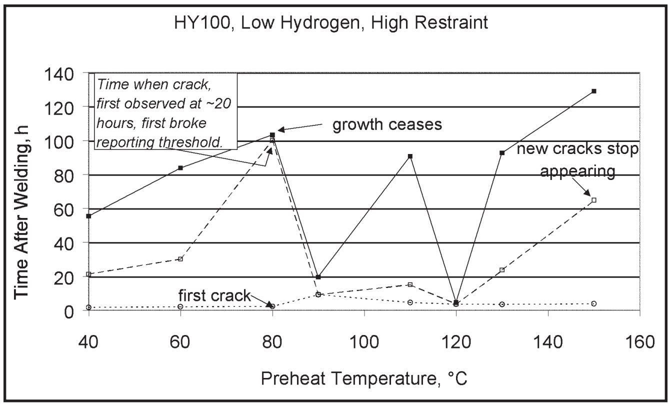

Fig. 6 — Delay time measurements for HY100, low-hydrogen, high-restraint groove welds.

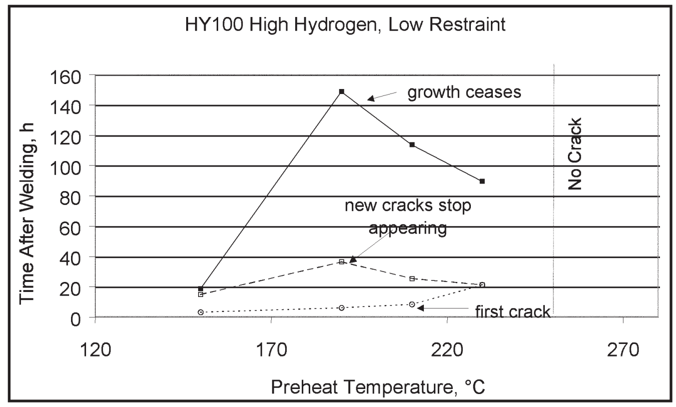

Fig. 7 — Delay time measurements for HY100, high-hydrogen, low-restraint groove welds.

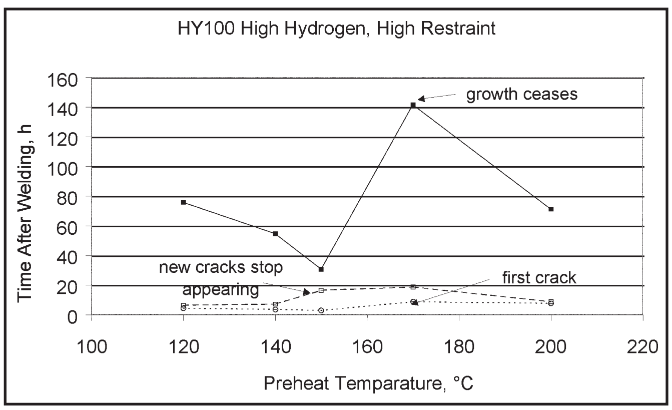

Fig. 8 — Delay time measurements for HY100, high-hydrogen, high-restraint groove welds.

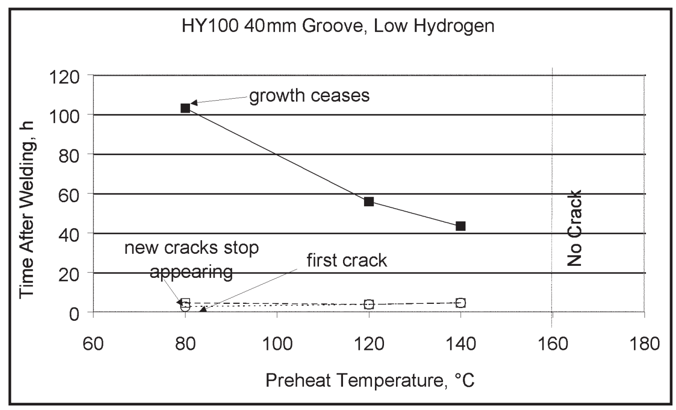

Fig. 9 — Delay time measurements for HY100, low-hydrogen, 40-mm-deep groove welds.

(80°C [176°F] preheat, Fig. 6) the crack that is recorded as appearing at 100 hours was actually present, but just below the reporting threshold, from about 20 hours. At 90°C (194°F) and 120°C (248°F) preheat (W1-42 and W1-46), only one crack was detected. Overall, the expected greater delay time near threshold cracking conditions was confirmed. Results indicated that a low-hydrogen, high-restraint weld in HY100 will result in the greatest delay time before the last initiation of discrete new cracks. The 40-mm groove welds appeared to result in the shortest delay times, and restraint had no clear effect on delay times.

The anticipated decrease in hydrogen diffusivity in the higher sulfur C-Mn steel did not have a measurable effect on delay times, but this was confused by the fact that this steel proved to be less hardenable (possibly because of its higher S content) despite having a marginally higher carbon equivalent, and cracking occurred in the weld metal, as opposed to HAZ cracking in the cleaner steel. There was also no measurable delay time for the 450-MPa steel welds at just below 1 kJ/mm (25 kJ/in.), which also cracked in the weld metal.

Although a particular series of groove welds was carried out to explore the effects of heat input, the effect is most clearly demonstrated by examining all C-Mn steel data (350-MPa and 450-MPa yield) together. These results are presented in Fig. 10, and it can be seen that there is a trend of increasing delay time with increasing heat input.

Superimposition of the Q1N data on the plot in Fig. 10 indicates that the results lay within the scatter of the C-Mn steel results. It should be recognized, however, that the cracking in this weld was in weld metal, which had a relatively lean composition and, particularly in view of the longer delay time observed in HY100 welds, it cannot be concluded that HAZ cracking in Q1N may not be subject to greater delays than in lower strength C-Mn steels.

The welds made in a wider groove did not show a measurable difference in time for crack initiation, with a maximum delay of 1 hour being recorded, by comparison with a value of 4 hours for similar heat input welds in a narrower groove. Crack growth was observed to continue for up to 11 hours, by comparison with 5 hours with the narrower groove.

Discussion

Material Effects

In the background section of this paper, variables likely to influence the tendency for hydrogen cracking to be delayed were identified based on the assumption that delayed cracking must be diffusion controlled. It was stated that delay times would be expected to be influenced by the diffusivity of hydrogen, the tendency for hydrogen to migrate to or remain at sites of high triaxial stress, and by the actual distance hydrogen is required to diffuse before it can concentrate sufficiently to cause cracking.

The most notable aspect of the results obtained was the very marked difference in behavior between the 350- and 450-N/mm^2 yield C-Mn steels and the higher strength, more highly alloyed 690-N/mm^2 yield HY100. Obviously there will be a significant difference between residual stress levels within weldments in the two materials. However, another very significant difference between these two steels and between the two weld metals used is the lower hydrogen diffusivity expected in a

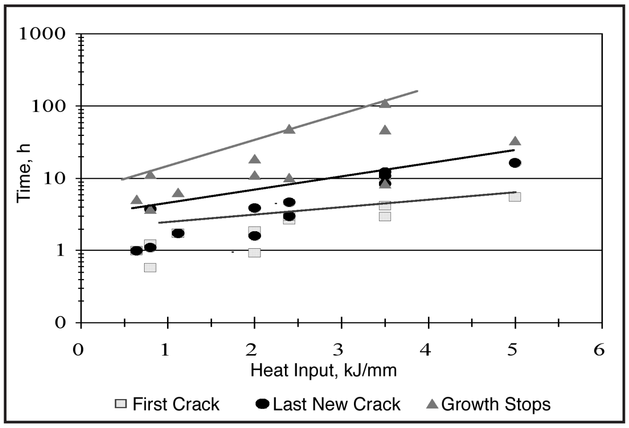

Fig. 10 — Summary of all 350-MPa and 450-MPa yield steel results.

more highly alloyed steel. Both a higher strength/residual stress level and a lower hydrogen diffusivity would be expected to result in longer delay times, but from these results, it is impossible to establish whether either of these is dominant. From the observation that the relatively lean Q1N weld metal showed delay times characteristic of the C-Mn steels, however, it would appear that diffusivity is more important than strength per se.

It is also discernible from published literature that delay time is greater for alloy steels. Interante and Stout (Ref. 10) found increasing delays on moving from A302 to HY80 to T-1 steels (Fig. 11), and Alcantara et al. (Ref. 11) similarly found increasing delays when welding C-Mn pipe with increasing strength consumables between 7018 and 13018.

It was expected that some delayed cracking might be observed in the welds made in the higher sulfur (and therefore possibly lower hydrogen diffusivity) C-Mn steel tested. As described in the results section, however, for this steel, cracking occurred only in the weld metal, which was of the same composition and diffusivity as used for the low-sulfur steel. The cleanliness of a C-Mn steel may, however, have an influence on delayed HAZ cracking, which was not detected in this program. It should also be noted, however, that high-sulfur C-Mn steels do not necessarily have lower hydrogen diffusivities (Ref. 12).

Hydrogen Level and Restraint

Although the results revealed marked difference in delay times observed between the two main steel types (C-Mn and low alloy), very little difference in delayed cracking behavior was seen as hydrogen level and restraint were varied in each case. For the C-Mn steel, the limited amount of delayed growth that did occur was only seen in high-restraint welds. However, the HAZ cracking in these welds was replaced by weld metal cracking in the low-restraint and deep groove welds which cracked without measurable delay, making it difficult to discern whether the type of cracking or the restraint level was responsible for the lack of delayed crack growth. The behavior of the HY100 welds, which showed only very small differences in delayed cracking behavior between high and low hydrogen levels and between high and low restraint, indicate that these factors are indeed of little significance. The very limited effect of hydrogen level upon crack delay times is not, perhaps, surprising for alloy steels when the concepts of risk of hydrogen cracking and risk of delayed cracking are separated. This is because for cracking to occur in any given weld, the hydrogen level at the time and place where it occurs will be constant for a threshold condition since, in alloy steels, microstructural susceptibility varies very little. Thus, below a given hydrogen level, cracking will never occur, and above a given level, excess hydrogen will have evolved in order to achieve a threshold condition before the weld cools to a temperature where cracking can occur.

The fact that restraint seemed to have no effect upon delay times may be explained by the fact that the "low" restraint was not low enough to prevent near-yield-magnitude residual stresses developing in the weld. This is not unrealistic for fabrication welds, and so although it may be possible to increase delay times with artificially low levels of restraint (and therefore stress) in specially designed single-pass test welds, these are unlikely to be relevant to real welds. For example, the low-restraint Lehigh tests performed by Interrante and Stout (Ref. 10), in which delay times were seen to increase as restraint decreased, rely upon a stress-concentrating root notch to induce longitudinal HAZ or weld metal cracking. This test is therefore largely insensitive to longitudinal residual stresses, and the transverse restraint (and, therefore, transverse residual stress) had to be lowered to levels untypical of a real fabrication before delayed cracking was observed.

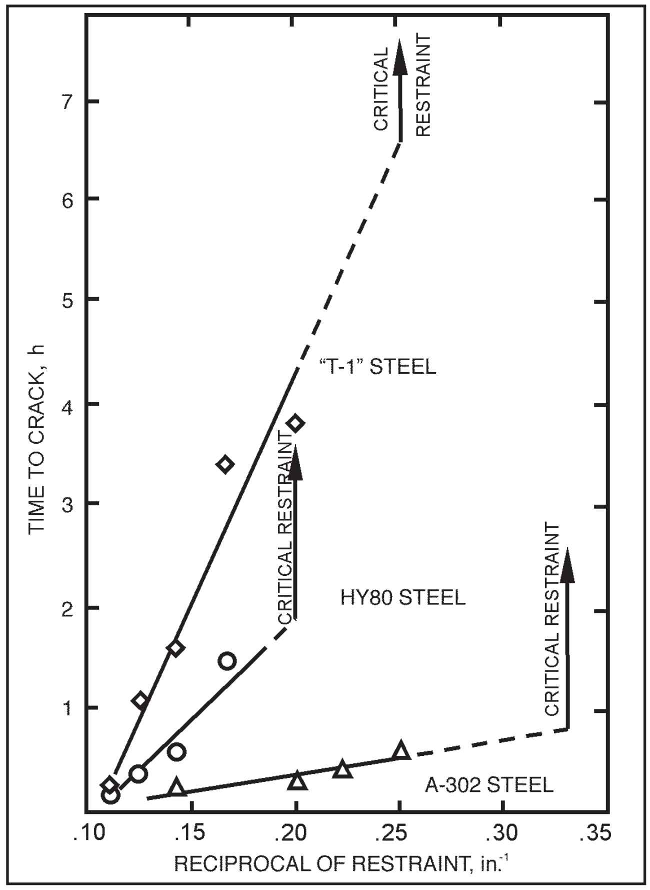

Fig. 11 — Effect of steel type on delay time. After Interante and Stout (Ref. 10).

Joint Thickness and Weld Volume

Joint thickness appeared to have no effect with the C-Mn steel and the surprising effect of reducing delay times at greater thickness with the HY100. A greater weld thickness would be expected to increase delay times because bulk hydrogen concentration will decay only very slowly from the center of thick sections. The slightly reduced delay times seen in this work between 20-mm- and 40-mm- (0.8- and 1.6-in.-) deep welds in HY100 may be explained by the fact that the thicker welds took longer to complete and were therefore at the preheat/interpass

Table 1 — Chemical Compositions of Base Materials

Element wt-%	Low-Sulfur C-Mn Steel	High-Sulfur C-Mn Steel	450 N/mm² QT Steel	450 N/mm² Yield Steel	HY100	Q1N Steel
C	0.19	0.18	0.09	0.06	0.17	0.13
S	<0.002	0.037	<0.002	0.003	0.002	<0.002
P	0.021	0.018	0.010	0.010	0.008	0.009
Si	0.28	0.45	0.41	0.18	0.28	0.23
Mn	1.38	1.57	1.23	1.47	0.28	0.29
Ni	0.01	0.04	0.50	0.76	2.89	2.88
Cr	0.02	0.02	0.02	0.02	1.59	1.25
Mo	<0.005	0.01	0.17	<0.005	0.51	0.4
V	<0.002	0.002	0.05	0.002	<0.002	<0.002
Cu	0.005	0.06	0.01	0.23	0.13	0.02
Nb	0.024	0.047	<0.002	0.015	<0.002	<0.002
Ti	0.002	<0.002	0.004	0.014	0.004	0.003
Al	0.047	0.045	0.030	0.058	0.024	0.019
O	0.0004	0.0035	0.0009	—	0.014	—
N	0.0041	0.0076	0.0055	—	0.0096	—
CE_{IIW}[(a)]	0.43	0.45	0.38	0.38	—	0.70
Ca	—	—	—	0.0012	—	<0.0003

(a) $CE_{IIW} = C + Mn/6 + (Cr + Mo + V)/5 + (Ni + Cu)/15$.

Table 2 — Chemical Compositions of Weld Metals

Element wt-%	E7018	SD3 SAW	SD3 1Ni-¼Mo SAW	E8018 G	E12018 M	E9016 G
C	0.11	0.08	0.06	0.10	0.11	0.05
S	0.008	0.003	0.005	0.006	0.008	0.005
P	0.011	0.018	0.016	0.008	0.010	0.011
Si	0.44	0.33	0.24	0.41	0.43	0.35
Mn	1.65	1.49	1.34	1.62	1.58	1.44
Ni	0.02	0.04	0.99	0.97	2.25	0.82
Cr	0.03	0.03	0.02	0.02	0.55	0.03
Mo	0.005	<0.005	0.48	<0.005	0.49	0.20
Cu	0.01	0.20	0.19	0.03	0.03	0.01
V	0.01	0.002	0.002	0.01	0.01	0.002
Nb	0.002	0.005	<0.002	<0.002	<0.002	<0.002
Ti	0.008	0.002	0.004	0.005	0.006	0.029
Al	<0.003	0.012	0.014	0.003	<0.003	0.016

Table 3 — Summary of Test Series

Hydrogen:	High	High	Low	Low	Low	SAW
Restraint:	High	Low	High	Standard	Standard	
Groove Depth:	20 mm	20 mm	20 mm	40 mm	40 mm	
Groove Angle:	2×10 deg	2×10 deg	2×10 deg	2×30 deg	2×10 deg	
350-MPa Yield, Clean	0.8–1.1	0.8	0.56–0.8	0.8	1.1	5.0
350-MPa Yield, Dirty			0.7-0.8			
450-MPa Yield			0.7–0.8, 2.0–2.4			3.5
HSLA (Q1N)			2.0			
Low Alloy (HY100)	1.1	1.1	1.1		1.1	

Note: Range of heat input (kJ/mm) employed given where tests were carried out.

temperature or above for a longer period, allowing hydrogen to accumulate at sites of high triaxial stress during welding. It is therefore likely that had the weld been completed more quickly with higher arc energies and thus greater bead sizes, the delay times may have been increased rather than reduced. It should also be recognized that the increase in joint thickness was achieved by machining a deeper groove, which made hydrogen-escape from the root of the weld (through the reverse face) easier. Nevertheless, the results of tests made in a wider (60-deg included angle) groove also showed no measurable effect on delay time. Overall, it is evident that extrapolation of results to different weld geometries and procedures must be done with caution.

Effect of Heat Input

One of the clearest effects to come out of this work is that of heat input. The results plotted in Fig. 10 indicate that the upper bounds of all three parameters (first observation of a crack, last appearance of a new crack, and end of crack growth) increase measurably over the range 0.8–5 kJ/mm. Although there is no overlap between the 3.5–5 kJ/mm welds made using submerged arc and the 0.7–2.4 kJ/mm welds made using shielded metal arc, the effect is observable in both groups, and one bounding line can be drawn for both sets, indicating that this is a heat input effect and not a process effect.

Relation to Other Work

As well as enabling guidance to be given on appropriate delay time before inspection, this work has produced results that are largely in agreement with previous published work on delayed cracking and, to a certain extent, explain a large amount of the anecdotal evidence of delayed cracking. A common feature of delayed cracking reported in the literature is rapid crack initiation followed by significantly more prolonged periods between bursts of growth (Refs. 6, 8, and 13). This type of behavior has also been seen in this work and has significant implications for inspection procedures, as previously mentioned, as well as explaining the very long delay times sometimes reported when only surface inspection is used. In this work, crack initiation was seen to occur as long as 65 hours after welding (in HY100), but in the majority of cases, all detectable cracks were present within 24 hours, even when growth was seen to continue for more than 100 hours. Thus, it is highly probable that in many cases where delay times in excess of 24 hours have been reported before cracks are first detected, this has been due to the

Table 4 — Results of Delay Time Measurements

Specimen	Heat input, kJ/mm / preheat, °C	Time after end of welding when test starts, h	Temp. at start of test, °C	Time taken to reach ambient, h	Time after which cracking is first noticed[(a)], h	Temp. after which cracking is first noticed, °C	Time up to which new defects start appearing, h	Time up to which defect growth occurs, h
a) Low-hydrogen – high-restraint welds, clean 350-MPa steel								
W1-14	0.56/20	0.66	35.3	11.3	0.66	35.3	0.66	0.66
W1-10	0.64/20	1.00	24.0	8.9	1.00	24.0	1.00	5.14
W1-18	0.72/20	1.00	27.5	9.8	1.00	27.5	1.00	1.00
W1-28	0.80/20	1.23	23.5	7.2	1.23	23.5	3.78	3.78
W1-30	0.80/20	1.38	27.5	6.1	—	—	—	—
b) High-hydrogen – high-restraint welds, clean 350-MPa steel								
W1-11	0.80/20	1.25	26.9	9.6	1.25	26.9	1.25	1.25
W1-16	0.96/20	2.35	30.4	12.4	2.35	30.4	2.35	2.35
W1-20	1.12/20	1.75	27.3	9.7	1.75	27.3	1.75	6.4
c) High-hydrogen – low-restraint welds, clean 350-MPa steel								
W1-25	0.80/20	1.08	25.4	9.3	1.08	25.4	1.08	1.08
W1-26	0.80/40	0.70	28.0	9.2	0.70	28.0	0.70	0.70
W1-29	0.80/50	1.2	27.4	6.1	—	—	—	—
W1-27	0.80/60	2.08	27.2	10.4	—	—	—	—
d) Low-hydrogen – 40-mm-deep groove – high-restraint welds, clean 350-MPa steel								
W1-62	1.12/55	1.33	30.2	6.0	1.33	1.33	1.33	1.33
W1-61	1.12/70	2.13	27.8	8.7	—	—	—	—
e) Low-hydrogen – high-restraint welds, 690-MPa low-alloy steel (HY100)								
W1-2	1.12/40	1.66	30.0	9.8	1.66	30.0	21.3	>55.4[(b)]
W1-8	1.12/60	2.00	24.9	7.1	2.00	24.9	30.2	83.8
W1-15	1.12/80	2.25	28.3	11.3	2.25	28.3	100.0	103.2
W1-42	1.12/90	3.38	27.0	12.2	9.15	21.5	9.15	19.5
W1-48	1.12/110	3.97	28.0	13.9	4.49	25.2	15.0	90.6
W1-46	1.12/120	3.55	26.4	9.2	3.55	26.4	3.55	4.55
W1-49	1.12/130	3.38	29.7	16.0	3.38	29.7	23.7	92.6
W1-50	1.12/150	3.82	29.6	15.5	3.82	29.6	64.8	129.0
f) High-hydrogen – high-restraint welds, low-alloy steel (HY100)								
W1-19	1.12/120	4.31	28.4	13.2	4.31	28.4	6.34	75.7
W1-22	1.12/140	3.50	29.9	15.1	3.50	29.9	7.10	54.6
W1-23	1.12/150	2.33	31.9	14.0	2.83	28.8	16.5	30.6
W1-37	1.12/170	5.07	27.9	13.6	8.67	22.0	18.6	141.6
W1-51	1.12/200	4.03	26.5	13.5	7.63	23.0	8.71	71.7

continued

Note: Welds are listed in lowest crack risk condition last.
(a) If cracking is detected on the first inspection, it is the same as the time after welding when the tests start.
(b) Inspection stopped due to an equipment problem.

time taken for either subsurface cracks to break surface and become detectable with a surface technique such as MPI or for buried cracks to grow to a detectable size by less sensitive NDE techniques such as radiography.

Although very long delay times similar to those previously reported have been seen in this work, the phenomenon of delayed cracking has, nevertheless, been shown to be restricted to particular welding situations. Conditions must be such that sufficient hydrogen can be introduced that will later just cause cracking when it concentrates, without there being so much hydrogen as to result in immediate cracking as the weld cools to ambient. This work indicates that such conditions are relatively rare but are more likely to occur with high-strength, low-diffusivity steels such as HY100. This again is in agreement with previous experience. The majority of reported delay in cracking has been in high-strength steels (Refs. 6, 10, 11, and 14).

An exception to this is the reported delay in cracking observed in the high-arc-energy submerged arc welded C-Mn steel (Ref. 13) confirmed by the present work. In this case the particular circumstances required for delayed cracking are thought to arise because of the greater diffusion distances resulting in longer diffusion times rather than lower diffusivity. This observation is very significant as it suggests that bead size/heat input is an important variable affecting delay times.

Delay Times for Inspection in Fabrication

The purpose of this work was to provide better supported, and thus both more cost effective and safer, guidelines for delays to be imposed between completion of welding and inspection for fabrication hydrogen cracks. Some consideration should be given to the possibility that the detectability of cracks may not always be as good in practice, and particularly during site work, as achieved during the laboratory work, even though reasonably realistic levels of detectability have been adopted in the present work. Nevertheless, the results for C-Mn steels do indicate that there is significant scope for reduction in delay times before inspection.

Table 4 continued — Results of Delay Time Measurements

Specimen	Heat input, kJ/mm / preheat, °C	Time after end of welding when test starts, h	Temp. at start of test, °C	Time taken to reach ambient, h	Time after which cracking is first noticed, h	Temp. after which cracking is first noticed, °C	Time up to which new defects start appearing, h	Time up to which defect growth occurs, h
g) High-hydrogen – low-restraint welds, 690-MPa low-alloy steel (HY100)								
W1-32	1.12/150	3.16	28.3	13.1	3.16	28.3	14.8	18.65
W1-33	1.12/170	5.38	26.1	16.3	—	—	—	—
W1-34	1.12/190	5.58	26.3	25.1	6.08	26.3	36.4	148.7
W1-35	1.12/210	5.76	27.0	27.9	8.30	23.0	25.4	113.64
W1-36	1.12/230	7.67	24.0	26.0	21.2	20.5	21.2	89.5
W1-38	1.12/250	4.91	29.7	27.9	—	—	—	—
h) Low-hydrogen – 40-mm-deep groove – high-restraint welds, 690-MPa low-alloy steel (HY100)								
W1-31	1.12/80	2.63	27.3	9.66	2.63	27.3	4.45	103.0
W1-39	1.12/120	3.73	27.1	10.46	3.73	27.1	3.73	55.8
W1-40	1.12/140	3.33	27.4	10.8	4.53	24.0	4.53	43.3
i) Low-hydrogen – high-restraint welds, high-sulfur 350-MPa steel								
W1-56	0.72/20	0.80	22.2	7.6	0.80	22.2	0.8	0.8
W1-52	0.80/20	0.75	0.9	7.2	0.75	23.9	7.5	7.5
W1-55	0.72/40	1.67	21.8	6.0	—	—	—	—
W1-54	0.80/40	1.65	27.5	11.5	—	—	—	—
j) Low-hydrogen – high-restraint welds, 450-MPa steel								
W1-57	0.80/20	1.16	22.3	7.5	1.16	22.3	1.16	1.16
W1-59	0.80/40	1.67	27.5	9.8	—	—	—	—
W1-58	0.80/60	2.25	27.4	9.5	—	—	—	—
W1-53	0.80/20	0.58	24.9	9.9	—	—	—	—
W2-2	2.0/20	1.33	29	16.1	1.33	29	1.33	1.33
W2-3	2.0/20	1.80	40	25.3	1.80	40	1.80	1.80
W2-4	2.0/20	0.93	29	15.9	0.93	29	1.60	18.7
W2-10	2.4/20	2.67	32	9.74	2.67	32	4.7	48.9
W2-11	2.4/20	3.00	32	9.25	—	—	—	—
W2-12	2.4/20	3.00	27	15.3	3.00	27	3.00	10.3
k) Submerged arc welds, clean 350-MPa steel								
W1-101	5.0/170	9.2	33.1	—	—	—	—	—
W1-102	5.0/170	7.3	24.0	—	—	—	—	—
W1-100	5.0/170	5.5	26.7	—	5.5	26.7	16.5	33.5
l) Submerged arc welds, 450-MPa steel								
W2-5	3.5/75	2.15	48	18.7	4.18	27	8.48	8.48
W2-8	3.5/95	2.95	41	22.5	2.95	41	12.32	110.0
W2-9	3.5/120	3.1	44	25.3	10.9	20	10.9	47.6
m) Low-hydrogen – high-restraint welds, 565-MPa HSLA steel (Q1N)								
W2-6	2.0/120	2.78	38	18.1	—	—	—	—
W2-7	2.0/90	1.97	40	18.1	—	—	—	—
W2-18	2.0/20	1.87	26	14.67	1.87	26	3.9	11.2
n) Low-hydrogen – high-restraint – wide groove welds, clean 350-MPa steel								
W2-13	0.8/20	0.5	32	8.57	0.50	32	0.50	0.50
W2-14	0.8/40	0.58	36	18.24	0.58	36	1.10	11.4
W2-15	0.8/60	1.00	34	17.33	—	—	—	—
W2-16	0.8/50	0.78	32	9.88	—	—	—	—
W2-17	0.8/40	0.63	32	10.57	—	—	—	—

For a total of 29 cracked tests for heat inputs up to and including 2.4 kJ/mm (61 kJ/in.) produced with SMAW, the greatest delay time has not exceeded 4.7 hours.

Proposed modifications to current practice for delay times before inspection for C-Mn steels of yield strength up to and including 450 N/mm^2 and of up to 50-mm thickness are given in Table 5 and incorporate a considerable safety factor. Although it is believed that the increase in delay times between shielded metal arc and submerged arc welds is an effect of heat input, it is considered appropriate, in the absence of other data, to restrict the greatest reduction in delay time (to 12 hours, compared with typical current practice, of 16–48 hours) for heat inputs of ≤ 2.4 kJ/mm (61 kJ/in.) to SMAW.

Measured delay times for high-strength steels such as HY100 were much larger than for the C-Mn-type materials, primarily due to the expected influence of the significant levels of alloying on hydrogen diffusivity. Thus, for these steels, at least 72 hours is recommended, and it must be recognized that crack growth may continue for some time beyond this.

A similar effect of heat input may also apply to the higher strength steel. However, while in practice, steels of the HY100 type are less likely to be welded at high heat inputs, further work would be re-

Table 5 — Guidelines for Delay Time before Inspection for C-Mn Steels of Yield Strength of up to and Including 450 N/mm^2 and up to 50 mm Thick

Arc Energy, kJ/mm (kJ/in.)	Heat Input, kJ/mm (kJ/in.)	Delay Time before Inspection (at an ambient temperature of 20°C [68°F])	
		Observed greatest delay time for crack initiation, h	Proposed ultrasonic inspection, h
≤ 3 (≤ 76)[(a)]	≤ 2.4 (≤ 61)[(a)]	4.7	12
≤ 3.5 (≤ 89)[(b)]	≤ 3.5 (≤ 89)[(b)]	12.3	24
3.5–5 (89–127)[(b)]	3.5–5 (89–127)[(b)]	16.5	36

(a) For SMAW only.
(b) For SAW only.

quired to investigate this factor for such steels.

The Q1N material is significantly more alloyed than the C-Mn steels studied in the present project, and it could be expected that it might produce delay times significantly longer than the C-Mn steels and similar to those observed for HY100. However, typical consumables for welding Q1N, such as the E9016G used, are significantly less highly alloyed than those used for HY100. This is considered to be the reason why the delay times observed were similar to those for C-Mn steels since the cracking produced in the Q1N tests was in the weld metal and not the HAZ. Thus, the data generated can only be considered relevant to detection of weld metal cracking when welding Q1N with the E9016G used or similarly alloyed consumables. Delay times for HAZ cracking in Q1N, based on the above considerations, would be expected to be longer because of the slower diffusivity of hydrogen in the more highly alloyed HAZ material. To a first approximation, they would be expected to be similar to those observed in HY100, based on the similar levels of alloying. However, hydrogen loss from the HAZ would, in fact, largely take place through the weld metal, where diffusivity, based on relative alloy levels, might be faster. Until such considerations are demonstrated, it is recommended that where there is concern over HAZ cracking in Q1N, normal practice for delay times should be followed.

In view of the relevance of hydrogen diffusion, the indications from the present results that thickness is not an important variable, within the range studied, should not be taken to mean that greater thickness has no effect on delay time. Therefore, the present results and recommendations should be considered to only apply to material of ≤ 50-mm (≤ 2-in.) thickness. Until proven otherwise by experiment, it should be anticipated that for significantly greater material thickness, longer delay time could be required. The importance of hydrogen diffusion indicates that a further variable, ambient temperature, should be considered. Although the question of ambient temperature has not been addressed in this work, it is very likely that lowering ambient temperature will increase delay times (Ref. 6). This should be borne in mind if welding is to be performed at temperatures below 20°C (68°F), and the possibility of longer delay times should be allowed for.

Conclusions

1. For C-Mn-type steels of up to 450-MPa (65-ksi) yield strength, delay times were found to increase with increasing heat input over the range studied of 0.7 to 5 kJ/mm.

2. Delay times for weld metal cracking when welding Q1N steel at a heat input of 2.0 kJ/mm with the E9016G used, or similarly alloyed consumables, were similar to those for C-Mn steels.

3. Significant delay times of up to 64 hours before the last initiation of a new crack and up to 140 hours before all subsequent crack growth ceases have been recorded for welds in the 690-MPa (100-ksi) yield strength steel. The longest time before detectable cracks were first produced was 21 hours.

4. Delay times before cracking in both the 350-MPa (51-ksi) yield C-Mn steel 1B789 and the 690-MPa (100-ksi) yield HSLA steel 1B778 appear to be largely insensitive to the variables restraint, hydrogen level, and weld thickness, within the ranges studied.

5. Increasing the weld volume (cross-sectional area) by changing the angle of preparation had no significant influence on delay times in a 350-MPa (51-ksi) yield strength steel.

6. Guidelines for delay times before inspection for hydrogen cracks have been produced. Seventy-two hours is recommended for 690-MPa (100-ksi) yield low-alloy steel welded at <1.1 kJ/mm heat input at 20°C (68°F) ambient temperature. Recommended delays for C-Mn steels are tabulated in Table 5.

References

1. British Standards Institution. *Welding — Recommendations for Welding of Metallic Materials — Part 2: Arc Welding of Ferritic Steels.* BS EN 1011-2:2001.

2. American Welding Society. AWS D1.1:2000*, Structural Welding Code — Steel. Miami Fla.*

3. DNV Rules for Classification of Fixed Offshore Installations, Part 3.

4. Construction Specification for Fixed Offshore Structures in the North Sea. EEMUA 158, 1994 revision.

5. *National Structural Steelwork Specification for Building Construction,* 3d ed. BCSA and SCI publication No. 203/94, July 1994.

6. Beacham, E. P., Johnson, H. H., and Stout, R. D. 1961. Hydrogen and delayed cracking in steel weldments. *Welding Journal* 40(4): 155-s to 159-s.

7. Andersson, B. A. B. 1982. Hydrogen induced crack propagation in a QT steel weldment. *Journal of Engineering Materials and Technology* 104(4) (October): 249–256.

8. Troiarno, A. R. 1960. The role of hydrogen and other interstitials in the mechanical behaviour of metals. *Transactions of the ASM* 52: 54–80.

9. Bailey, N., Coe, F. R., Gooch, T. G., Hart, P. H. M., Jenkins, N., and Pargeter, R. J. 1993. *Welding Steels without Hydrogen Cracking,* 2d ed. Abington Publishing.

10. Interrante, C. G., and Stout, R. D. 1964. Delayed cracking in steel weldments. *Welding Journal* 43(4): 145-s to 160-s.

11. Alcantara, N. G., Oliveras, J., and Rogerson, J. H. 1984. Non-destructive testing in the fitness-for-purpose assessment of welded constructions. *Proceedings International Conference,* London, Nov. 20–22. The Welding Institute.

12. Hart, P. H. M. 1978. Low sulphur levels in C-Mn steels and their effect on HAZ hardenability and hydrogen cracking. *International Conference on Trends in Consumables for Welding.* London, Nov. 14–16. The Welding Institute.

13. Böhme, D., and Eisenbeis, C. 1980. Untersuchungen über die verzögerte Rissbildung am beispiel von querrissen im einlagigen unterpulverschweissgut von feinkorn baustählen. *Schweissen und Schneiden* 32(10): 409–413.

14. Juers, R. H. 1982. Determination of intra and post-weld hydrogen removal thermal soaking treatments for HY-130/MIL-14018 SMAW weldments. *First International Conference on Current Solutions to Hydrogen Problems in Steels.* Washington, D.C., Nov. 1–5. Materials Park, Ohio: ASM International.